

Low to high shear rate powder rheology in a rotational rheometer

A. Zharbossyn¹, S. Mahdavy^{2,*}, D. Barletta¹, L. Orefice³, V. Magnanimo⁴, S. Luding², and M. Poletto¹

¹ Dipartimento di Ingegneria Industriale, Università degli Studi di Salerno, Fisciano (SA), Italy

² Multi-Scale Mechanics (MSM), Thermal and Fluid Engineering, Faculty of Engineering Technology, University of Twente, Enschede, Netherlands

³ MercuryLab B.V., Enschede, Netherlands

⁴ Soil MicroMechanics (SMM), Civil Engineering and Management, Faculty of Engineering Technology, University of Twente, Enschede, Netherlands

Abstract. Characterization techniques are essential for understanding powders' complex behavior. Among different devices, the Anton Paar Powder Rheometer (MCR-302) was used to characterize high-density polyethylene (HDPE). The powder has a 214 μm median diameter and is classified as free-flowing. The rheometer measures the torque required to rotate an impeller within the powder cell over a wide range of impeller rotation velocities from 0.6 rpm to 600 rpm. The steady-state torque dependence on the rotation velocities of the impeller follows a function (similar to shear thickening) as in the μ -I-rheology, reflecting that the torque is sensitive to inertial/viscous effects at higher rotation velocities (60 and 600 rpm) while quasi-static at lower rotation velocities (0.6 and 6 rpm). Our results indicate that the dry air fluidization at 600 rpm has a minimal effect on the steady-state torque.

1 Introduction

Powders are used in industrial applications in food, chemical, pharmaceutical, and metallurgical industries [1]. They play an important role in granulation, chemical reaction processes, mixing, storage and handling, and additive manufacturing [1,2]. In powders, each particle interacts with the others and the surrounding environment. They exhibit complex behavior that notably differs from simple solids or fluids [3,4]. Experimental and analytical techniques are required to understand powder flow and design and manage efficient and reliable industrial processes.

In addition, simulation-based techniques find widespread application in studying powder bulk properties, ranging from research to industrial uses. While experimental methods are established, numerical techniques are also becoming increasingly important in powder classification, equipment design, quality control, and troubleshooting [5]. The successful application of these techniques requires quantitative information on powder properties, such as flowability.

Various instruments and methods have been developed to measure powder bulk characteristics, ranging from traditional evaluation methods to advanced rheological instruments. Traditional methods such as the angle of repose, Hausner ratio, and shear cell testing have long been employed to analyze powder flowability and cohesion [5,6]. They are inexpensive and relatively easy to implement, but lack precision at low consolidation stresses [7] and provide results either limited to powder displacement or within a minimal range of slow shear rate in the case of shear testers – while being better controlled due to the finite confining stress [5].

More recently, newer instruments such as the FT4 Powder Rheometer and the Anton Paar Powder

Rheometer have become available, equipped to measure flow energy, torque, and other dynamic properties under controlled conditions and with a wide range of shear rates – complementary and coherent with different powder flow characterization procedures [4,7]. Such modern, automated instruments can provide a comprehensive view of powder behavior at much broader shearing conditions. A wealth of data that has an excellent potential for the validation of numerical techniques and for a deeper insight into the flow of particulates, which, however, requires a complete understanding of the several mechanisms appearing even in a simple testing procedure.

In this study, we highlight the effect of several key testing parameters using the Anton Paar Powder Rheometer with a high-density polyethylene (HDPE) powder.

2 Experimental procedure

2.1 Anton Paar Powder Rheometer

The Anton Paar Powder Rheometer (MCR-302) is designed to measure the bulk flow properties of powders. It quantifies the torque required to rotate an impeller inside a powder bed in a cell. The powder cell consists of a cylindrical vessel (50 mm diameter) with a uniform and porous ceramic gas distributor at the base. The high-pressure drop through the ceramic distributor ensures a uniform gas distribution, irrespective of the bed state and even for fine powders [7,8]. This setup includes mass flow controllers that enable precise aeration of the powder bed, allowing experiments at different conditions, ranging from no aeration to complete fluidization. The torque measurement is performed by immersing an impeller in the powder,

* Corresponding author: s.mahdavy@utwente.nl

fixed at a particular vertical position, and rotating at a specified revolutions per minute (rpm). Fig. 1 shows the experimental cell in two states: empty and filled with powder.

The torque measurement in the Anton Paar Powder Rheometer yields results at rotational velocities ranging from 0.06 rpm to 600 rpm. At low shear rates comparable to shear testing, the measured torque depends on the internal friction and cohesion of the powder, which is influenced by material properties, impeller position, and aeration rate [7,8]. In this research, we employed a wide range of impeller rotational velocities, spanning from 0.6 rpm to 600 rpm, and two different aeration rates.

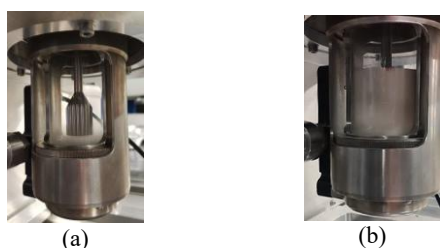


Fig. 1. Anton Paar Powder Rheometer cell: (a) empty cell, (b) cell filled with the powder.

A grooved impeller, as shown in Fig. 1a, is used in this research. The specialized concave grooves on the impeller surface retain powder, avoiding surface slip behavior. The impeller's vertical position is fixed, ensuring a 22 mm gap between the cell bottom and the impeller base.

2.2 Powder

A high-density polyethylene (HDPE) powder, with a median size of 214.6 μm , was utilized in the rheometer cell. Shear testing experiments on this powder classify it as a free-flowing powder. Table 1 illustrates the detailed properties of the powder.

Table 1. HDPE powder properties. The table includes density (ρ_p) and diameters of the 10th, 50th, and 90th percentiles of the particle size distribution.

Property	Value
ρ_p (kg/m ³)	950
d_{10} (μm)	113.0
d_{50} (μm)	214.6
d_{90} (μm)	391.8

2.3 Procedure

Before the experiments, the powder was dried in an oven, and then 43.6 g of the powder was poured into the cell. For all measurements, the following protocol steps were applied to all powder samples: 1) drying in an oven, cooling in a desiccator, 2) pouring it into the cell, 3) fluidizing with dry air, 4) stopping fluidization and resting for 10 seconds, and 5) measuring the torque with no airflow.

3 Results and discussion

In the following subsections, we present results investigating the effects of the impeller inertia, the preconditioning fluidization step, and the rotational velocity on the measured torque.

3.1 Impeller inertia effect

To understand the effect of the impeller inertia, we conducted two experiments: one in a powder-filled cell and the other in an empty cell. Fig. 2a displays the measured torque obtained in these experiments by rapidly bringing the impeller to the set rotational speed as shown in Fig. 2b. In both experiments, the torque reaches its peak and then falls to nearly zero, as visualized in the inset of Fig. 2a. After that, in the cell containing the powder, the torque increases again, eventually reaching a steady-state. Similar fluctuations are visible for the empty cell before the signal stabilizes at approximately zero. Such fluctuations are likely due to the impeller's natural elastic oscillations triggered by the high initial acceleration.

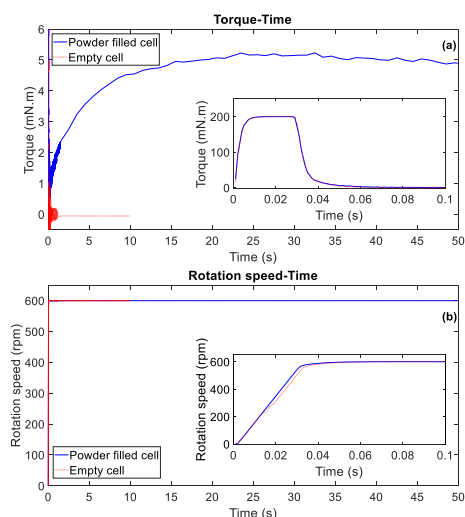


Fig. 2. a) Measured torque and b) imposed rotational velocity in the empty cell and the presence of a powder. Insets show a closer view between 0 and 0.1 s.

3.2 Effect of aeration in preconditioning

As mentioned in Section 2.3, the powder is fluidized inside the cell with dry air. The fluidization helps to remove the powder's history. To assess the effectiveness of this step, we employed air flow rates of 12 L/min and 14 L/min, along with fluidization periods ranging from 60 to 120 seconds. Fig. 3 displays the torque measured in step 5 for different preconditioning conditions. The results closely match, despite slight differences in onset and peak values. Preconditioning with larger air flow rates and longer fluidization times slightly increases the measured torque.

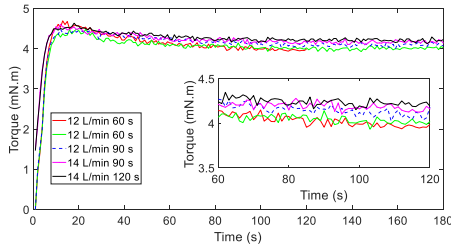


Fig. 3. Time series of the measured torque for HDPE powder at 600 rpm for different conditions of preconditioning fluidization (legend); inset shows a zoom-in.

3.3 Powder Rheology: effect of rotational speed

Fig. 4 shows the impeller’s torque over time at four different impeller rotational velocities, ranging from fast (600 rpm) to slow (0.6 rpm), obtained in a bed of 43.6 g of HDPE preconditioned by 120 s of fluidization at an air flow rate of 12 L/min.

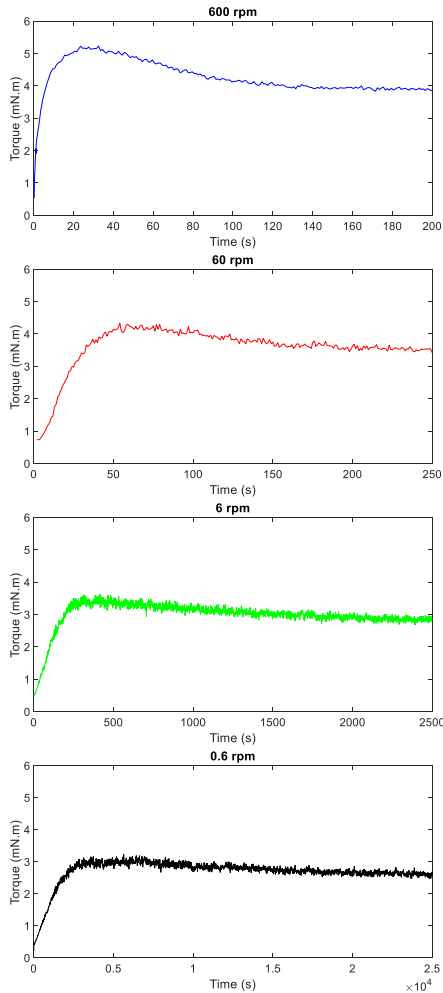


Fig. 4. Torque time series for different impeller rotational velocities for a bed of 43.6 g of HDPE preconditioned by 120 s of fluidization at an air flow rate of 12 L/min.

In the time series, at all impeller velocities, the torque increases, then shows a peak, and slowly decreases to a steady-state value. Both the torque peak and the steady-state values decrease as the impeller’s rotational velocity decreases. However, the time required to reach steady-state decreases with the rotational velocity.

Using strain instead of time to plot the torque series provides a more significant comparison between the experiments, assuming that the changes induced in the bed by the impeller rotation are mostly due to the imposed deformation. The strain, δ , at the impeller surface, the maximum in the system, is calculated as:

$$\delta = f \frac{2\pi}{60} t \quad (1)$$

where f and t are, respectively, the rotational frequency in rpm and time in seconds.

Fig. 5 shows the torque plotted as a function of the strain for different rotational velocities. Note that for 600 rpm, additional data beyond 1600 rad have been excluded to visualize the results at low strain better. The torque values at lower rotation speeds (0.6 and 6 rpm) are close to each other. However, increasing the rotation speed from 6 rpm to 60 rpm has a significant impact on the torque in both the overshoot and steady-state regions. The powder at 600 rpm exhibits the highest torque.

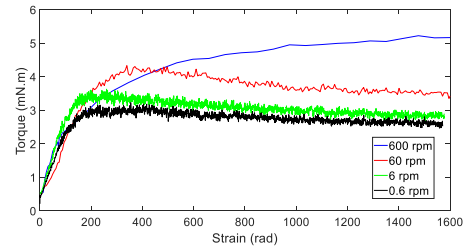


Fig. 5. Torque vs strain for data in Fig. 4.

In the low-speed regime (0.6–6 rpm), the torque response exhibits weak rate dependence, suggesting that viscous contributions are minor and elastic solid-like behavior with irreversible plastic rearrangements dominates the powder’s response. The observed rate effects may result from a combination of intrinsic material viscosity and extrinsic inertial effects at high speeds (60–600 rpm). Given the non-cohesive behavior of the 200 μm particulate, the effect of rate-dependent micro/nano-scale interactions (e.g., van der Waals or capillary forces) is negligible, supporting a primarily frictional and contact-based deformation mechanism.

To investigate the rheological behavior of the granular material, the friction coefficient (μ) and inertial number (I) are derived from measured torque values and rotational speeds. The pressure within the granular bed is estimated based on hydrostatic pressure by the solid phase. For conciseness, the detailed calculation procedure can be found in Reference [9]. This approach enables the evaluation of μ and I under various experimental conditions. Table 2 shows the measured torque values used to calculate the inertial number and friction coefficient at each rotational speed. The data are then fitted using the $\mu(I)$ rheological model, expressed as:

$$\mu = \mu_0 + \frac{\mu_\infty - \mu_0}{I_0 I + 1} \quad (2)$$

As illustrated in Fig. 6, the best-fit parameters are $\mu_0 = 0.80$, $\mu_\infty = 1.22$, and $I_0 = 0.003$. These values demonstrate a reasonably good agreement with the experimental data. For example, the low-shear friction coefficient μ_0

underestimates the friction obtained from the Schulze Ring Shear Tester [10].

$$\mu_0 = \tan(40^\circ) = 0.84 \quad (3)$$

Moreover, the fitted transition parameter I_0 aligns well with the commonly accepted threshold between quasi-static and intermediate flow regimes. This threshold also supports the observation that the transition in the regimes occurs between 6 to 60 rpm, as shown in the Fig. 5.

Table 2. Averages and standard deviation of steady-state torque, with calculated inertial number and bulk friction, at different rotational velocities for a bed of 43.6 g of HDPE, preconditioned by 120 s of fluidization at an air flow rate of 12 L/min.

f (rpm)	\bar{T} (mN.m)	σ (mN.m)	I (-)	μ (-)
0.6	2.585	0.048	8×10^{-5}	0.80
6	2.853	0.053	8×10^{-4}	0.89
60	3.529	0.054	8×10^{-3}	1.10
600	3.878	0.030	8×10^{-2}	1.21

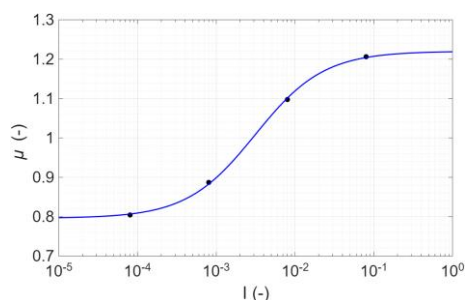


Fig. 6. Bulk friction as a function of Inertial number. The points show the experimental data, and the blue line shows the regressed Eq. (2), where $\mu_0 = 0.80$, $\mu_\infty = 1.22$, and $I_0 = 0.003$.

4 Conclusion

The Anton Paar Powder Rheometer was tested on a free-flowing HDPE powder at a wide range of shear rates. This device measures the torque required for impeller rotation inside a preconditioned powder bed. The effects of impeller inertia, fluidization conditions in the preconditioning step, and impeller rotational velocity on the torque were investigated. Results indicate that the fluidization air flow rate and duration in powder preconditioning have only minor effects on the steady-state torque, while the impeller rotational velocity significantly impacts the torque in both transient and steady-state, with this effect being more pronounced at higher rotational speeds. Impeller inertia has to be considered for the initial instants of the rheometer response.

This study was conducted using free-flowing powder. Further analysis is required for additional experiments on cohesive powders. Preliminary results indicate further challenges due to non-repeatable measurements, possibly resulting from issues with caking and inhomogeneous stress distributions, which prevented precise and easy-to-interpret rheological measurements.

Future work will focus on calibrating DEM interaction parameters for various materials and across different testers [10] that complement each other. DEM simulations will also help better understand possible secondary flows inside the rheometer.

Acknowledgements

This research is part of the TUSAIL project (<https://tusail.eu>) and has received funding from the European Horizon 2020 Framework Programme for research, technological development, and demonstration under grant agreement ID 955661.

We would like to pay our deepest gratitude and respect to our late colleague, Assem Zharbossyn, who passed away in January 2023. Her experimental results form the foundation of this research. We are honored to continue her scientific legacy and commemorate her contributions to this field.

References

- [1] B. Jadidi, M. Ebrahimi, F. Ein-Mozaffari, A. Lohi, A comprehensive review of the application of DEM in the investigation of batch solid mixers, *Reviews in Chemical Engineering* 39, 729 (2023).
- [2] S. Z. Ajabshir, D. Barletta, M. Poletto, The Effect of Process Conditions on Powder Flow Properties for Slow Flow Regimes, *KONA Powder and Particle Journal* 42, 2025006 (2025).
- [3] V. Francia, L. Ait Ali Yahia, R. Ocone, A. Ozel, From Quasi-static to Intermediate Regimes in Shear Cell Devices: Theory and Characterisation, *KONA Powder and Particle Journal* 38, 2021018 (2021).
- [4] W. Nan, M. Ghadiri, Y. Wang, Analysis of powder rheometry of FT4: Effect of air flow, *Chem Eng Sci* 162, 141 (2017).
- [5] D. Barletta, M. Poletto, A. C. Santomaso, Bulk Powder Flow Characterisation Techniques, in *Powder Flow: Theory, Characterisation and Application*, edited by A. Hassanpour, C. Hare, M. Pasha (The Royal Society of Chemistry, 2019), pp. 64–146.
- [6] J. Schwedes, Review on testers for measuring flow properties of bulk solids, *Granul Matter* 5, 1 (2003).
- [7] H. Salehi, D. Barletta, M. Poletto, D. Schütz, R. Romirer, On the use of a powder rheometer to characterize the powder flowability at low consolidation with torque resistances, *AIChE Journal* 63, 4788 (2017).
- [8] M. Lupo, D. Schütz, E. Riedl, D. Barletta, M. Poletto, Assessment of a powder rheometer equipped with a cylindrical impeller for the measurement of powder flow properties at low consolidation, *Powder Technol* 357, 281 (2019).
- [9] L. A. A. Yahia, T. M. Piepke, R. Barrett, A. Ozel, and R. Ocone, Development of a virtual Couette rheometer for aerated granular material, *AIChE Journal* 66, (2020).
- [10] A. Zharbossyn, S. Mahdavy, D. Barletta, M. Poletto, V. Magnanimo, S. Luding, L. Orefice, A framework for upscaled particle calibration with powder characterization techniques, in preparation (2025).